



OPEN ACCESS

EDITED BY

Ruth Anne Eatock,
The University of Chicago, United States

REVIEWED BY

Takashi Nakamura,
Kyoto Prefectural University of
Medicine, Japan
Ebenezer N. Yamoah,
University of Nevada, Reno, United States

*CORRESPONDENCE

Kimberlee P. Giffen
✉ Kimberlee.giffen@uga.edu
David Z. He
✉ DavidHe@creighton.edu

RECEIVED 23 May 2024

ACCEPTED 27 September 2024

PUBLISHED 17 October 2024

CITATION

Giffen KP, Liu H, Yamane KL, Li Y, Chen L,
Kramer KL, Zallocchi M and He DZ (2024)
Molecular specializations underlying
phenotypic differences in inner ear hair cells
of zebrafish and mice.
Front. Neurol. 15:1437558.
doi: 10.3389/fneur.2024.1437558

COPYRIGHT

© 2024 Giffen, Liu, Yamane, Li, Chen, Kramer,
Zallocchi and He. This is an open-access
article distributed under the terms of the
[Creative Commons Attribution License \(CC
BY\)](https://creativecommons.org/licenses/by/4.0/). The use, distribution or reproduction in
other forums is permitted, provided the
original author(s) and the copyright owner(s)
are credited and that the original publication
in this journal is cited, in accordance with
accepted academic practice. No use,
distribution or reproduction is permitted
which does not comply with these terms.

Molecular specializations underlying phenotypic differences in inner ear hair cells of zebrafish and mice

Kimberlee P. Giffen^{1,2,3*}, Huizhan Liu³, Kacey L. Yamane³, Yi Li^{3,4},
Lei Chen⁵, Kenneth L. Kramer³, Marisa Zallocchi³ and
David Z. He^{3*}

¹Department of Neuroscience and Regenerative Medicine, Medical College of Georgia at Augusta University, Augusta, GA, United States, ²Department of Basic Sciences, Augusta University/University of Georgia Medical Partnership, Athens, GA, United States, ³Department of Biomedical Sciences, Creighton University School of Medicine, Omaha, NE, United States, ⁴Department of Otorhinolaryngology, Beijing Tongren Hospital, Beijing Capital Medical University, Beijing, China, ⁵Department of Cell and Developmental Biology, Vanderbilt University, Nashville, TN, United States

Introduction: Hair cells (HCs) are the sensory receptors of the auditory and vestibular systems in the inner ears of vertebrates that selectively transduce mechanical stimuli into electrical activity. Although all HCs have the hallmark stereocilia bundle for mechanotransduction, HCs in non-mammals and mammals differ in their molecular specialization in the apical, basolateral, and synaptic membranes. HCs of non-mammals, such as zebrafish (zHCs), are electrically tuned to specific frequencies and possess an active process in the stereocilia bundle to amplify sound signals. Mammalian HCs, in contrast, are not electrically tuned and achieve amplification by somatic motility of outer HCs (OHCs).

Methods: To understand the genetic mechanisms underlying differences between adult zebrafish and mammalian HCs, we compared their RNA-seq-characterized transcriptomes, focusing on protein-coding orthologous genes related to HC specialization.

Results: There was considerable shared expression of gene orthologs among the HCs, including those genes associated with mechanotransduction, ion transport/channels, and synaptic signaling. However, there were some notable differences in expression among zHCs, OHCs, and inner HCs (IHCs), which likely underlie the distinctive physiological properties of each cell type. For example, OHCs highly express *Slc26a5* which encodes the motor protein prestin that contributes to OHC electromotility. However, zHCs have only weak expression of *slc26a5*, and subsequently showed no voltage-dependent electromotility when measured. Notably, the zHCs expressed more paralogous genes including those associated with HC-specific functions and transcriptional activity, though it is unknown whether they have functions similar to their mammalian counterparts. There was overlap in the expressed genes associated with a known hearing phenotype.

Discussion: Our analyses unveil substantial differences in gene expression patterns that may explain phenotypic specialization of zebrafish and mouse HCs. This dataset also includes several protein-coding genes to further the functional characterization of HCs and study of HC evolution from non-mammals to mammals.

KEYWORDS

hair cells, gene orthologs, RNA-seq, transcriptome, prestin, zebrafish, mouse, hearing

Introduction

Hair cells (HCs) are the sensory receptors of the auditory and vestibular systems in the inner ear of all vertebrates. HCs transduce mechanical stimuli, i.e., movement in their environment, into electrical activity (1). The site of such mechano-electrical transduction is the stereocilia bundle, the hallmark of all HCs. In addition to the hair bundle on the apical membrane, the basolateral and synaptic membranes of HCs have structural and functional specializations which are responsible for electrical activities and synaptic transmission.

Even though mechanotransduction in the hair bundle is a shared feature of all HCs, there are profound differences in morphological and functional specializations between HCs of non-mammals and mammals. The HCs of non-mammalian species, such as fish and birds, enhance their auditory sensitivity and frequency selectivity via an electrical resonance shaped by voltage-gated ion channel activity and an active, force-generation process in the stereocilia bundle (2–5). Mammals have evolved two morphologically and functionally distinct HC types, the inner HCs (IHCs) and the outer HCs (OHCs). In contrast to non-mammals, the mammalian cochlear HCs are not electrically tuned, but rather accomplish the high sensitivity and frequency selectivity of hearing by using the mechanically tuned basilar membrane and prestin-based somatic motility of OHCs to amplify mechanical signals in the cochlea (6–8). The morphological and physiological differences among vertebrate HCs are still being explored. Comparison of the transcriptomic signatures underlying phenotypic specializations of non-mammalian and mammalian HCs can further our understanding of the molecular mechanisms underlying these differences.

Previously, we isolated pure populations of adult zebrafish inner ear HCs and adult mouse IHCs and OHCs for RNA-seq-based transcriptomic analyses (9, 10). To analyze the molecular differences among these HC populations, the transcriptomic datasets were refined to include only protein-coding gene orthologs. Our previous study identified 17,498 protein-coding gene orthologs in zebrafish which correspond to 13,557 orthologous mouse genes (11). This study aimed to characterize the expressed genes either common or unique to the HCs of each species, focusing on the genes known to encode HC specializations in the apical, basolateral, and synaptic membranes, since these genes should largely be responsible for phenotypical differences between zebrafish and mammalian HCs. Additionally, we compared expression of genes with a known association to hearing loss. Genes encoding transcription factors were also examined to elucidate pathways regulating expression of these protein-coding gene orthologs. Our transcriptome analyses are expected to serve as a highly valuable resource, not only for unraveling the molecular mechanisms of the unique biological properties of zebrafish and mouse HCs, but also to further our understanding of HC evolution from lower vertebrates to mammals.

Materials and methods

Zebrafish and mouse protein-coding gene orthologs

The built-in Ensembl Biomart package was used to access the annotated Ensembl Genes database (release 91) (12) to generate a list of zebrafish and mouse protein-coding gene orthologs. The Biomart classification and quality of orthologs incorporates a gene order conservation, both up and downstream of the gene of interest, whole genome alignment, and conservation of nucleotide sequences to predict high confidence orthology thresholds (13). The annotated gene lists for this study were based on the Zebrafish (*Danio rerio*) GRCz10 and mouse (*Mus musculus*) GRCm38 genome builds. In the zebrafish-to-mouse comparison, the zebrafish genes were filtered based on protein-coding function and homology with mouse genes, producing a total of 17,498 orthologs. Similarly, a mouse-to-zebrafish comparison identified a total of 13,526 protein-coding gene orthologs. The final mouse gene list included fewer orthologs because redundant genes corresponding to multiple zebrafish paralogs were removed from the gene list for analysis.

RNA-seq datasets

Previously published RNA-seq datasets were used in the comparative analysis of expressed protein-coding genes. Adult *Tg(pou4f3:GAP43-GFP)s273t* zebrafish inner ear HCs and non-sensory supporting cells (SCs) were collected using a unique suction pipette technique and isolated RNA was sequenced for transcriptomic analysis (9, 14, 15) (NCBI SRP113243). Similarly, isolated populations of IHCs and OHCs from 1-month-old CBA/J mouse cochleae were collected and utilized for RNA-seq analysis (10) (NCBI SRP133880).

The quantified cell-type specific gene expression data from these previous studies and the protein-coding gene ortholog lists were merged into a single dataset, which is provided as a searchable Excel table (Supplementary Data Sheet 1). The arbitrary expression value of 0.1 RPKM (Reads per kilobase per million mapped reads) (FDR p -value ≤ 0.10) was set as the minimum expression cutoff for both species. The expression values presented herein are not quantitatively equivalent, but rather are indicative of relative expression in mouse and zebrafish inner ear cell populations and thus should not be compared as absolute values. No custom code was used in this analysis.

Gene enrichment analysis

Differential gene expression among the HC populations was analyzed using iDEP 2.01 with DESeq2 (16), and volcano plots were generated to show up and downregulated genes (n = number of genes; \log_2 fold change > 1.0 ; $-\log_{10}$ adjusted p -value < 0.05). To further characterize the functions of groups of commonly or uniquely expressed gene orthologs, gene enrichment analysis was

conducted using ShinyGO v 0.80 (17). This web-based program utilizes the annotated Gene Ontology (GO) and other databases to provide enrichment analysis results. The p -value was set at < 0.05 .

Validation of gene expression

RT-PCR: A number of genes were selected for verification by RT-PCR based on shared or differential expression in zebrafish and mouse HCs. The oligonucleotide primers were designed with A plasmid Editor (ApE) software to find unique and appropriate sequences (18). Cell populations were collected using previously published protocols (9, 15). Total RNA was isolated using the Qiagen miRNeasy kit and quantified using a nanodrop spectrophotometer. The cDNA libraries were prepared from isolated RNA with the iSCRIPT reverse transcription supermix (Bio-Rad). RT-PCR reactions were prepared as 20 μ l reactions using 2x Master mix (Bio-Rad). All primers (Appendix 1) were acquired from Integrated DNA Technologies (Coralville, Iowa). Mouse stria cells and zebrafish non-sensory SCs were included as controls.

smFISH: To examine mRNA expression of select genes in the adult zebrafish and mouse inner ear epithelia, we used the RNAscope-based single molecule fluorescent *in situ* hybridization (smFISH) assay from Advanced Cell Diagnostics (ACD). Samples were pretreated according to the ACD protocol for formalin-fixed paraffin-embedded tissue. The pretreatment target retrieval and protease steps were slightly modified to prevent tissue damage. Tissues were covered with freshly prepared 0.5% pepsin +5 mM HCl in deionized water and incubated in the humidifying chamber at 37°C for 10 minutes. The remaining protocol was conducted according to the RNAscope 2.5 HD Detection Reagent RED user manual and published protocols (19). Following the final wash, samples were incubated with 4',6-diamidino-2-phenylindole (DAPI) to label nuclei. The smFISH probes were detected by red channel fluorescence (imaging described below), with no probe treatment included as a negative control.

Immunofluorescence: Mice (WT C57BL/6J) and zebrafish *Tg(Pou4f3:GFP)* were euthanized according to IACUC protocols. Mouse otic capsules and zebrafish inner ear tissues were dissected and placed in 4% paraformaldehyde (PFA) in 1X phosphate-buffered saline (PBS) for 24 h at 4°C. Following dissection for whole mount preparations, samples were washed in 1X PBS, then permeabilized and blocked in 1X PBS with 0.2% Triton X-100 (PBS-T) and 5% normal goat serum (NGS), followed by incubation with SLC7A14 primary antibody (Sigma:HPA045929; lot:R43519, 1:400) overnight at 4°C. Samples were rinsed in 1X PBS three times and then incubated with Alexa-Fluor (AF) conjugated secondary antibodies (Invitrogen) for 1 h at room temperature followed by subsequent washes. Additional staining with AF488-Phalloidin (anti-F-Actin) was used to label stereocilia. Finally, samples were rinsed three times in 1X PBS and mounted with SlowFade (Invitrogen), then imaged as below.

Confocal microscopy: Visualization of smFISH and immunofluorescence was conducted using Zeiss laser scanning confocal microscopes LSM700, 710, or 880. Sections were imaged

at 1.0 zoom at 40 \times or 63 \times magnification using Zen Black acquisition software. Additionally, samples for colocalization analyses, included cultured cells, were imaged on a Nikon Ti-E with a Yokogawa Spinning Disc Confocal with a Flash 4.0 Hamamatsu Monochrome camera.

Simultaneous recording of motility and nonlinear capacitance under voltage-clamp condition

Solitary HCs from zebrafish and mice were placed in the extracellular solution contained (mM): 120 NaCl, 20 TEA-Cl, 2 CoCl₂, 2 MgCl₂, 10 HEPES, and 5 glucose. Whole-cell voltage-clamp recordings were performed on an Olympus inverted microscope (IX71) with DIC. The patch pipette with the headstage of an Axopatch 200B amplifier (Axon Instruments) was held by a Narashige 3D micromanipulator (MHW-3). Whole cell voltage-clamp tight-seal recordings were established. The patch electrodes were pulled from 1.5 mm glass capillaries (WPI) using a Flaming/Brown Micropipette Puller (Sutter Instrument Company, Model P-97). Recording pipettes had open tip resistances of 4–5 M Ω and were filled with an internal solution that consisted of (mM): 140 CsCl, 2 MgCl₂, 10 EGTA, and 10 HEPES. The osmolarity and pH for both intracellular and extracellular solutions were adjusted to 300 mOsm/l and 7.3. The access resistance typically ranges from 8 to 14 M Ω after the whole-cell recording configuration was established. Voltage error due to the uncompensated series resistance was compensated off-line. All experiments were performed at room temperature ($22 \pm 2^\circ\text{C}$).

Motility and NLC were acquired simultaneously as described elsewhere (20). The AC technique was used to obtain motility-related gating charge movement and the corresponding non-linear membrane capacitance (21). In brief, it utilized a continuous high-resolution (2.56 ms sampling) two-sine voltage stimulus protocol (10 mV for both 390.6 and 781.2 Hz), with subsequent fast Fourier transform-based admittance analysis. These high frequency sinusoids were superimposed on staircase voltage (in 4 mV steps) stimuli. The evoked capacitive currents were filtered at 5 kHz and digitized at 100 kHz using jClamp software (SciSoft Company), running on an IBM-compatible computer and a 16-bit A/D converter (Digidata 1322, Molecular Devices). Motility was measured and calibrated by a photodiode-based measurement system (22) mounted on the Olympus inverted microscope. The magnified image of the edge of the cell was projected onto a photodiode through a rectangular slit. Somatic length changes, evoked by voltage stimuli, modulated the light influx to the photodiode. The photocurrent response was calibrated to displacement units by moving the slit a fixed distance (0.5 μ m) with the image of the cell in front of the photodiode. After amplification, the photocurrent signal was low-pass filtered by an anti-aliasing filter before being digitized by a 16-bit A/D board (Digidata 1322, Molecular Devices). The photodiode system had a cutoff (3 dB) frequency of 1,100 Hz. The motile responses were filtered at 1,100 Hz and digitized at 100 kHz. The voltage dependence of the cell length change also fits with the two-state Boltzmann function

and can be described as:

$$L = \frac{L_{\max}}{1 + \exp[-\alpha (V_m - V_{1/2})]}$$

where L_{\max} is the maximal length change, $V_{1/2}$ is the voltage at which $L = 0.5 L_{\max}$, α is the slope factor indicating the voltage sensitivity of the length change. Slope function was obtained as the derivative of the Boltzmann function. The non-linear capacitance can be described as the first derivative of a two-state Boltzmann function relating non-linear charge movement to voltage (23, 24). The capacitance function is described as:

$$C_m = \frac{Q_{\max} \alpha}{\exp[\alpha (V_m - V_{1/2})] (1 + \exp[-\alpha (V_m - V_{1/2})])^2} + C_{lin}$$

Results

Orthologous relationships of zebrafish and mouse protein-coding genes

A direct comparison of zebrafish and mouse protein-coding genes was conducted using Ensembl Biomart, based on the zebrafish GRCz10 and mouse GRCm38 gene assemblies (12). The analysis revealed a high number of orthologous genes shared among the two species (Table 1). Among the total zebrafish protein-coding genes, almost 70 percent had at least one mouse ortholog. The total number of orthologous zebrafish genes is greater as a result of a known ancient genome duplication event, so there were redundant mouse genes mapped to paralogous zebrafish genes (i.e., many-to-one, many-to-many) (25). The one-to-one zebrafish-to-mouse orthologs accounted for 39 percent of the zebrafish protein-coding genes. Furthermore, 3,248 of these genes were identified as high-confidence orthologs, with a gene order conservation score of ≥ 75 and/or whole genome alignment score of ≥ 75 and a percent identity score of ≥ 50 .

Commonly and uniquely expressed protein-coding gene orthologs among zebrafish and mouse inner ear HC populations

An initial comparison of the number of expressed protein-coding gene orthologs in the zHCs showed that 10,995 of the 17,498 orthologs were detected above the cutoff expression value of 0.10 RPKM (FDR p -value ≤ 0.10) (Figure 1B). Of the 13,526 mouse gene orthologs, 8,547 were expressed in IHCs, while 8,863 were expressed in OHCs (Figure 1B). Further comparison showed that a total of 6,659 genes were commonly expressed among all sensory HCs, with an additional 932 zebrafish gene paralogs (Figure 1A). There were 149 genes (+25 paralogs in zebrafish) commonly expressed in zHCs and IHCs, while there were 322 genes (+77 paralogs in zebrafish) expressed in zHCs and OHCs. The

TABLE 1 Classification of orthologous protein-coding genes.

Relationship	Zebrafish	Mouse
One-to-one	9,864	
One-to-many	6,723	3,425
Many-to-many	911	237
Ortholog total	17,498	13,526
Unique	7,600	8,532
Protein-coding gene total	25,098	22,058

mouse IHCs and OHCs shared a greater number of commonly expressed genes. The zHCs had the highest number of uniquely expressed genes (2,831), while the IHCs and OHCs expressed 145 and 288 unique genes, respectively. Differential gene expression analyses showed a greater number of upregulated genes in zHCs compared to IHCs or OHCs (Figures 1C, D). While the number of differentially expressed genes among IHCs and OHCs was notably lower (Figure 1E).

Enriched protein-coding gene orthologs expressed in zebrafish inner ear HCs compared to non-sensory zSCs

We analyzed differentially and uniquely expressed genes in zHCs with reference to non-sensory zSCs from the zebrafish inner ear since many of these genes may underlie specialization of sensory HCs. The top 200 gene orthologs uniquely expressed in zHC (zSCs ≤ 0.10 RPKM, FDR p -value ≤ 0.10) are shown in Figure 2A. Several of these genes are known to contribute to essential HC function in zebrafish including *chrna9a/b*, *lhflp5a*, *myo7aa*, *strc*, and *tmie* (4, 26). The top 200 upregulated, differentially expressed genes in zHCs (> 0.1 RPKM in zHCs and zSCs; Log2 fold change ≥ 1.0 ; FDR p -value ≤ 0.10) are shown in Figure 2B, with the fold-change in expression relative to the zSCs, shown to the right of each panel. Consistent with other studies, several of the top differentially expressed genes are pan-HC genes including *otofb*, *slc17a8*, and *ush1c* (26–28).

Gene ortholog expression among zHCs and mouse IHCs

Next, we examined similarities among the transcriptomic signatures of the primary auditory receptor cells in the mouse cochlea, IHCs, and their homolog in the zebrafish inner ear sensory epithelia. The top 200 expressed protein-coding orthologs in zHCs and IHCs are shown in Figures 3A, B, respectively. Among these top expressed genes, there were 47 genes commonly expressed in all HCs, 27 of which were one-to-one gene orthologs and 25 were ranked as high-confidence orthologs. Many of the highly expressed genes are associated with metabolic processes, including mitochondrial genes. Genes commonly expressed among the zHCs and IHCs including *anxa5a* (*Anxa5*), *pvalb8*, and *pvalb9* (*Ocm*) and *otofb* (*Otof*).

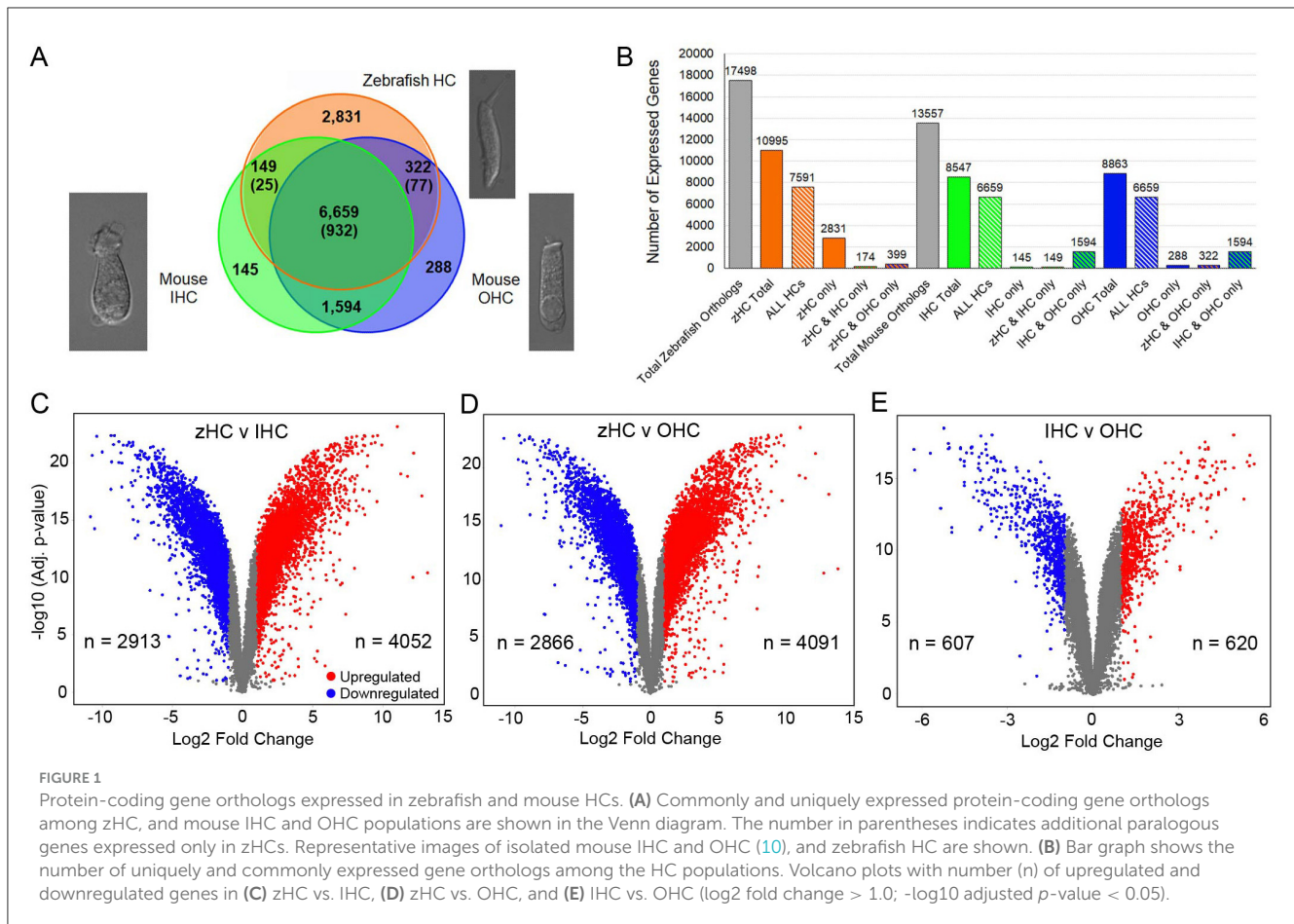


FIGURE 1

Protein-coding gene orthologs expressed in zebrafish and mouse HCs. (A) Commonly and uniquely expressed protein-coding gene orthologs among zHC, and mouse IHC and OHC populations are shown in the Venn diagram. The number in parentheses indicates additional paralogous genes expressed only in zHCs. Representative images of isolated mouse IHC and OHC (10), and zebrafish HC are shown. (B) Bar graph shows the number of uniquely and commonly expressed gene orthologs among the HC populations. Volcano plots with number (n) of upregulated and downregulated genes in (C) ZHC vs. IHC, (D) ZHC vs. OHC, and (E) IHC vs. OHC (\log_2 fold change > 1.0; $-\log_{10}$ adjusted p -value < 0.05).

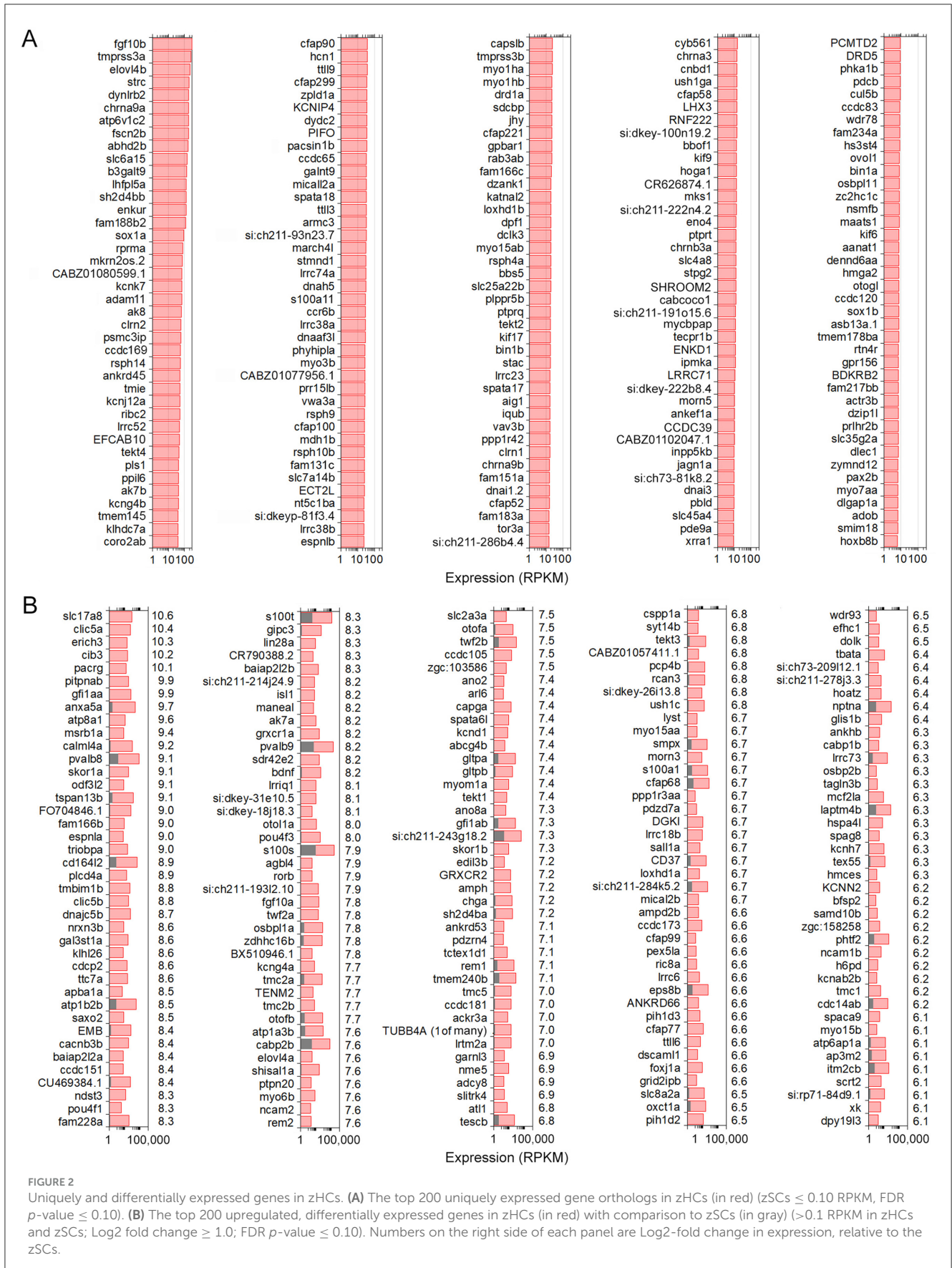
Expression of genes encoding functional HC proteins

Vertebrate HCs have specializations in the apical, basolateral, and synaptic membranes that are responsible for mechanotransduction, electrical and mechanical activities, and synaptic transmission. To examine expression of gene orthologs encoding proteins associated with the stereocilia bundle, we first generated a gene list based on two studies that examined proteins present in stereocilia bundles of mouse vestibular and chicken HCs using mass spectrometry (29, 30). Figure 4A shows expression levels of 113 gene orthologs, 45 of which are one-to-one orthologs, that encode stereocilia-associated proteins. As shown, 86 of the genes expressed in mammalian HCs are also expressed in zHCs, specifically those encoding the cytoskeletal structure and associated proteins. One-to-one gene orthologs highly expressed among all HC types included *arpc2*, *atp5b*, *capzb*, *cdc42*, *cfl1*, *fbxo2*, *gdi2*, *grxcr2*, *twf2b* (*Twf2*), and *ush1c*. Other distinctive patterns in gene expression among the HC populations were also identified. For example, *ldhba* (*Ldhb*) and *pvalb9* (*Ocm*) were highly expressed in all HCs, though notably, zHC and OHCs had higher expression than IHCs; *ldhba* (*Ldhb*) has been implicated in age-related hearing loss (31). *Actn4* and *Vill* were expressed only in IHCs and OHCs, not zHCs. Expression of both *capza1a* and *1b* was observed in zHCs, while *capzb* (*Capzb*) was highly expressed in all HCs. Finally, there was notable redundancy in expression of paralogous genes

in zHCs including *calm1a* and *b*, *dynll2a* and *b*, *pcdh15a* and *b*, etc.

Next, we further examined other HC function-associated genes, including those encoding components of the mechanotransduction apparatus (32). All HCs contain mechanotransduction channels in the stereocilia, including TMC1 (transmembrane channel-like 1) and/or TMC2 (33–35). LHFPL5, TMIE, and PIEZO2 are also necessary for mechanotransduction (36–39). As shown in Figure 4B, *Tmc1* (*tmc1*) is highly expressed in mouse HCs and zHCs. *Tmc2* is not detected in adult mouse HCs; however, both *tmc2a* and *tmc2b* are highly expressed in zHCs with expression values greater than *tmc1*. *Lhfp15* (*lhfp15a*) and *Tmie* (*tmie*) are expressed in mouse and zebrafish HCs, respectively.

HCs also contain various types of ion channels in the basolateral and synaptic membranes that are responsible for establishing and maintaining membrane potential, shaping receptor potentials, facilitating neurotransmitter release, and regulating cell volume (40, 41). Figure 4B includes expression of gene orthologs that encode various types of Cl^- , Ca^{2+} , Na^+ , and K^+ channels. Differential expression of several of these ion channel genes in IHCs and OHCs was previously observed in our RNA-seq analysis (15). There are some distinct differences in the expression of ion channel-related genes between zebrafish and mouse HCs. Zebrafish HCs have robust expression of *cacnb3b* (encoding voltage-dependent L-type calcium channel subunit beta-3), while mouse HCs have weak expression of *Cacnb3*. Conversely, robust



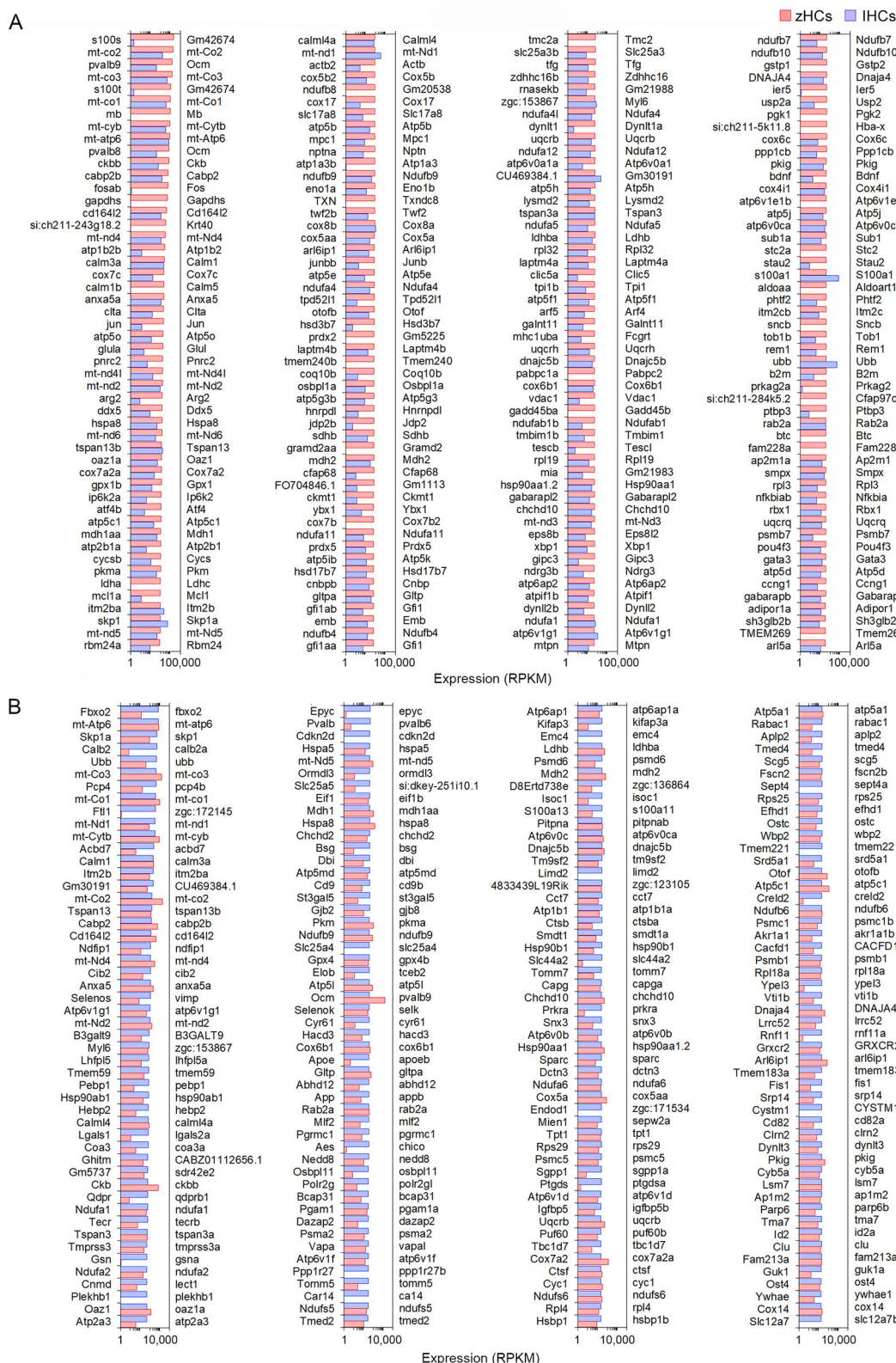
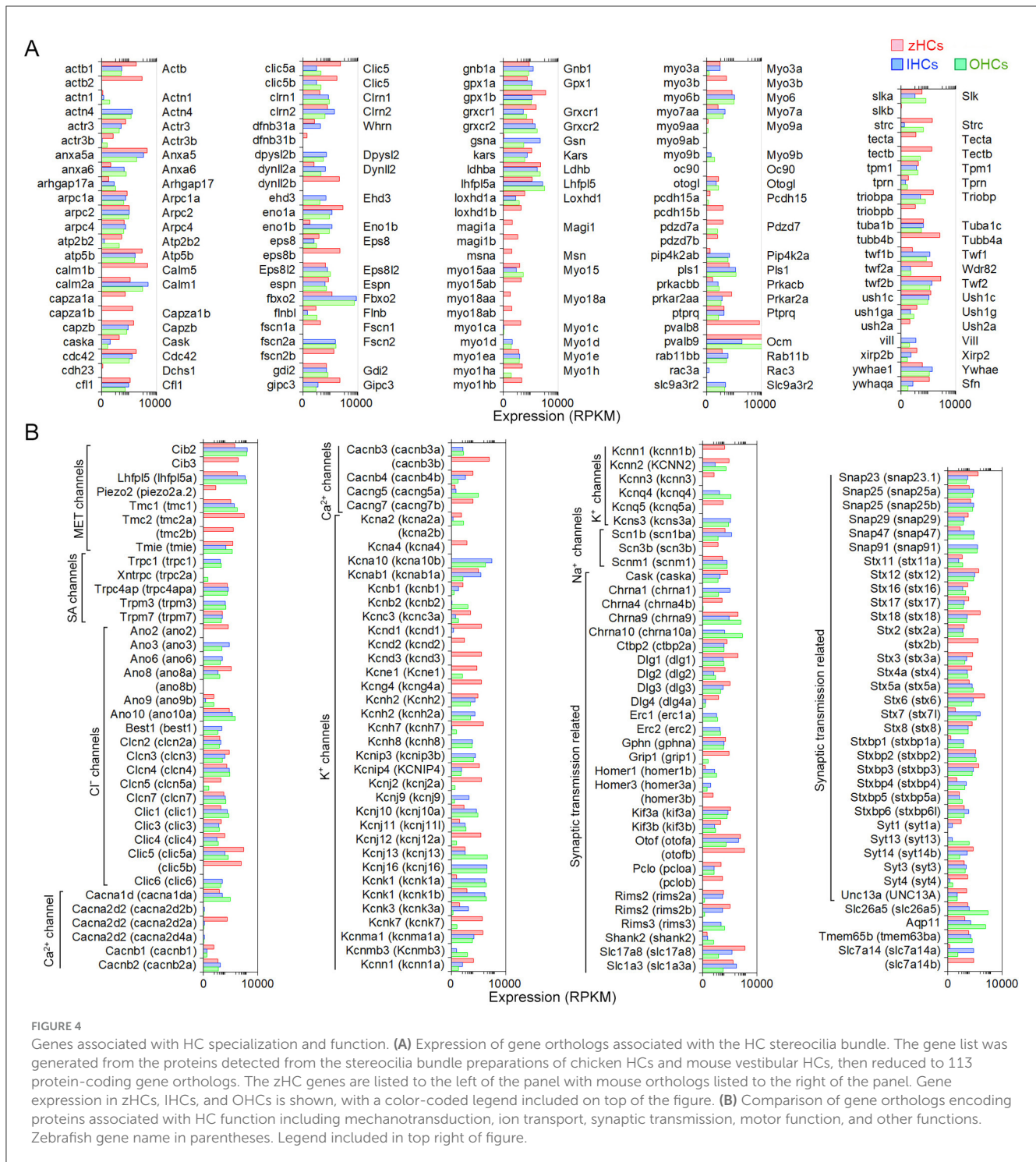


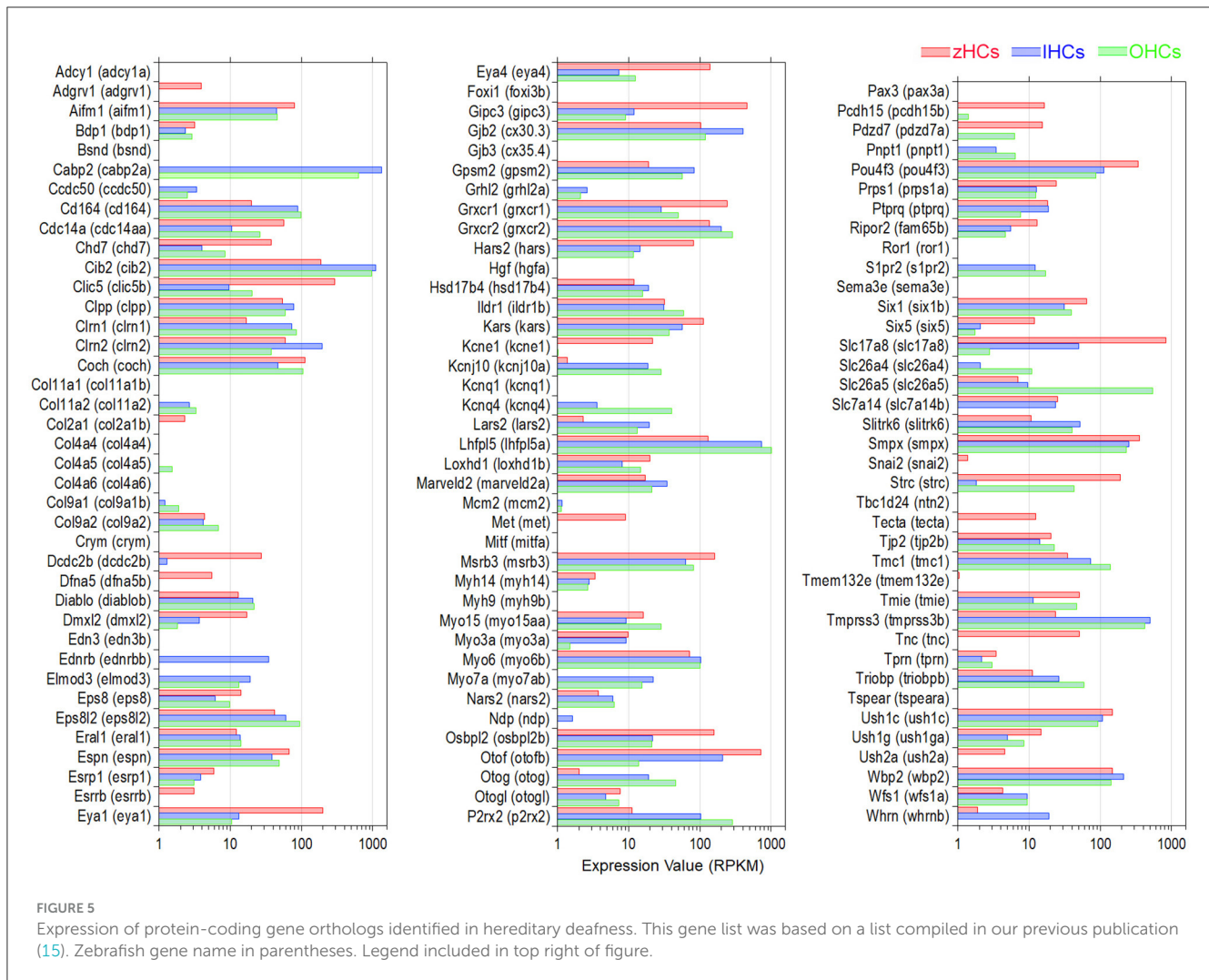
FIGURE 3
 Comparison of the top 200 protein-coding gene orthologs expressed in zHCs and mouse IHCs. **(A)** Top 200 expressed gene orthologs in zHCs (≥ 0.10 RPKM, FDR p -value < 0.10). Expression of gene orthologs in mouse IHCs (gene symbols listed on the right side of each panel) presented for comparison. **(B)** Top 200 gene orthologs expressed in IHCs (≥ 0.10 RPKM, FDR p -value < 0.10), with expression of the gene orthologs in zHCs presented for comparison. Note that direct comparison of normalized RPKM values is not reliable as the datasets for each species were analyzed independently. Legend included in top right of figure.



expression of *Cacna1d* (encoding voltage-dependent calcium channel, L type, alpha 1 subunit) and *Cacng5* (encoding voltage-dependent calcium channel, gamma subunit 5 or transmembrane AMPAR regulatory protein gamma-5) are detected in mouse HCs, especially in OHCs. Relatively high-level expression of *kcmd1*, *kcmd3*, *keng4a*, *kcnh7*, *kcnj12a*, *kcnk7*, *kcnma1a*, and *kcnq5a* is detected in zHCs. In contrast, robust expression of *Kcnj13* and *Kcnq4* is detected in OHCs, IHCs have relatively high expression of *Kcnh2*, *Kcnk1*, and *Kcns3*, and both express *Kcnj10*, *Kcnj16*, and

Kcnk1. Also, there was similar expression of *kcnab1a* (*Kcnab1*) in zHCs and IHCs, and *kcnm2* (*Kcnm2*) in zHCs and OHCs.

Finally, we examined expression of genes that encode proteins associated with pre-synaptic and post-synaptic mechanisms including pre-synaptic neurotransmitter vesicle transport and release, as well as post-synaptic nicotinic cholinergic receptors in zebrafish and mouse HCs. As shown in Figure 4B, the expression of genes encoding synaptic proteins is similar in zebrafish and mouse HCs, while differential expression of genes may underlie



distinct synaptic morphology and function of HC populations. For example, *Otof* (*otofa/b*) (42), *Slc17a8* (*slc17a8*) (43), and *Slc1a3* (*slc1a3a*) (9, 15) are more highly expressed in IHCs and zHCs. Interestingly, while both *Chrna9* (44) and *Chrna10* (45) are expressed in mouse HCs, especially OHCs, zHCs only express *chrna9*.

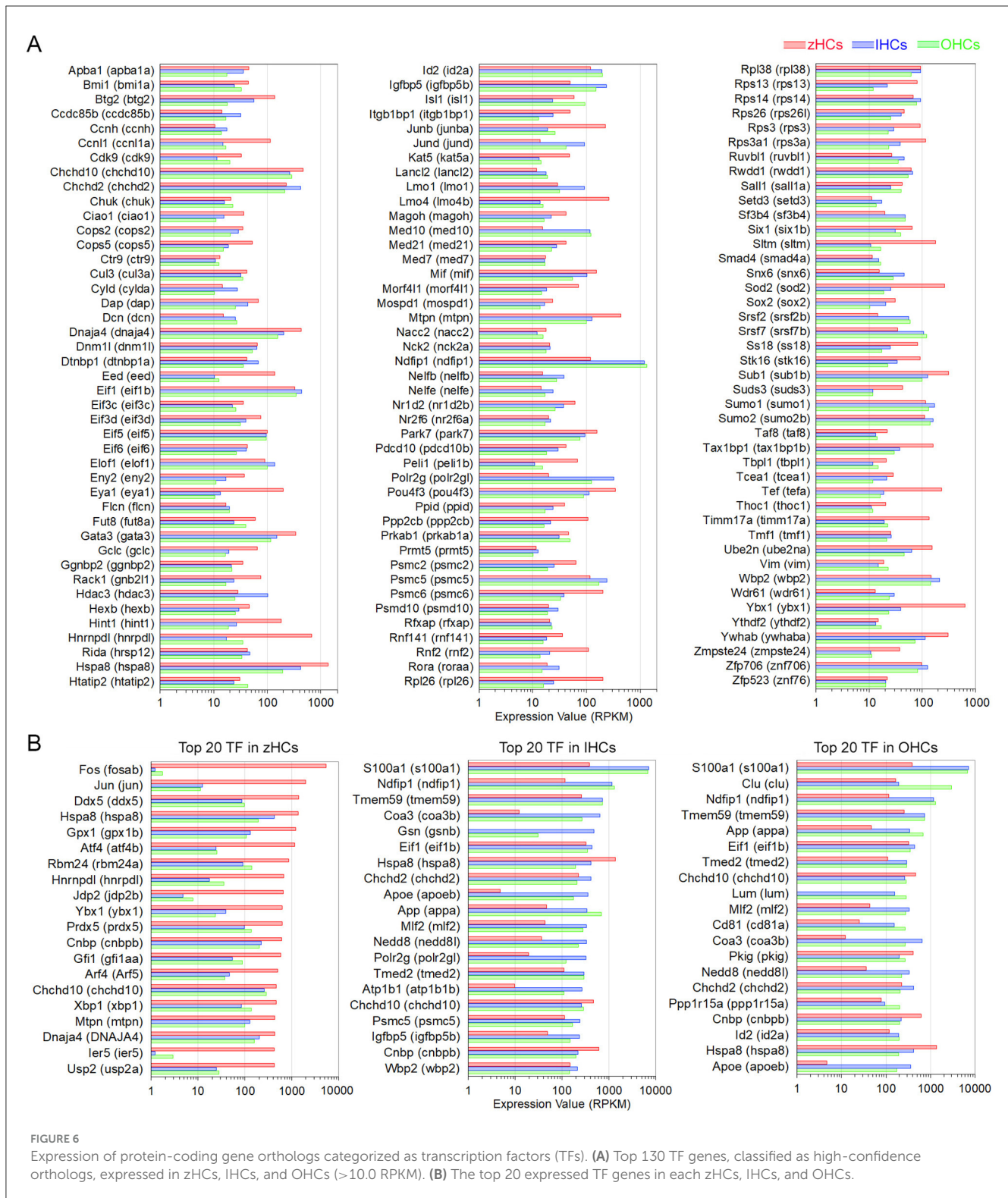
highly expressed in zHCs and OHCs. The orthologs *Slc17a8*, *Slc7a14* (*slc7a14b*), and *Otof* (*otofb*) were highly expressed in zHC and IHC.

Expression of gene orthologs associated with a hearing loss phenotype

A subset of genes associated with hearing loss phenotypes in humans, and experimentally validated in animal models, was compiled based on a list in our previous publication (15). Expression of 115 protein-coding mouse genes and corresponding zebrafish gene orthologs, 34 of which are classified as high confidence orthologs, is shown in Figure 5. There were several gene orthologs that were highly expressed in zHCs, IHCs, and OHCs including *Cib2*, *Gjb2* (*cx30.3*), *Grxcr2*, *Lhfp15* (*lhfp15a*), *Smpx*, and *Wpb2*. The gene ortholog *Strc*, encoding the stereocilin protein which forms horizontal connections in OHC stereocilia (46), was

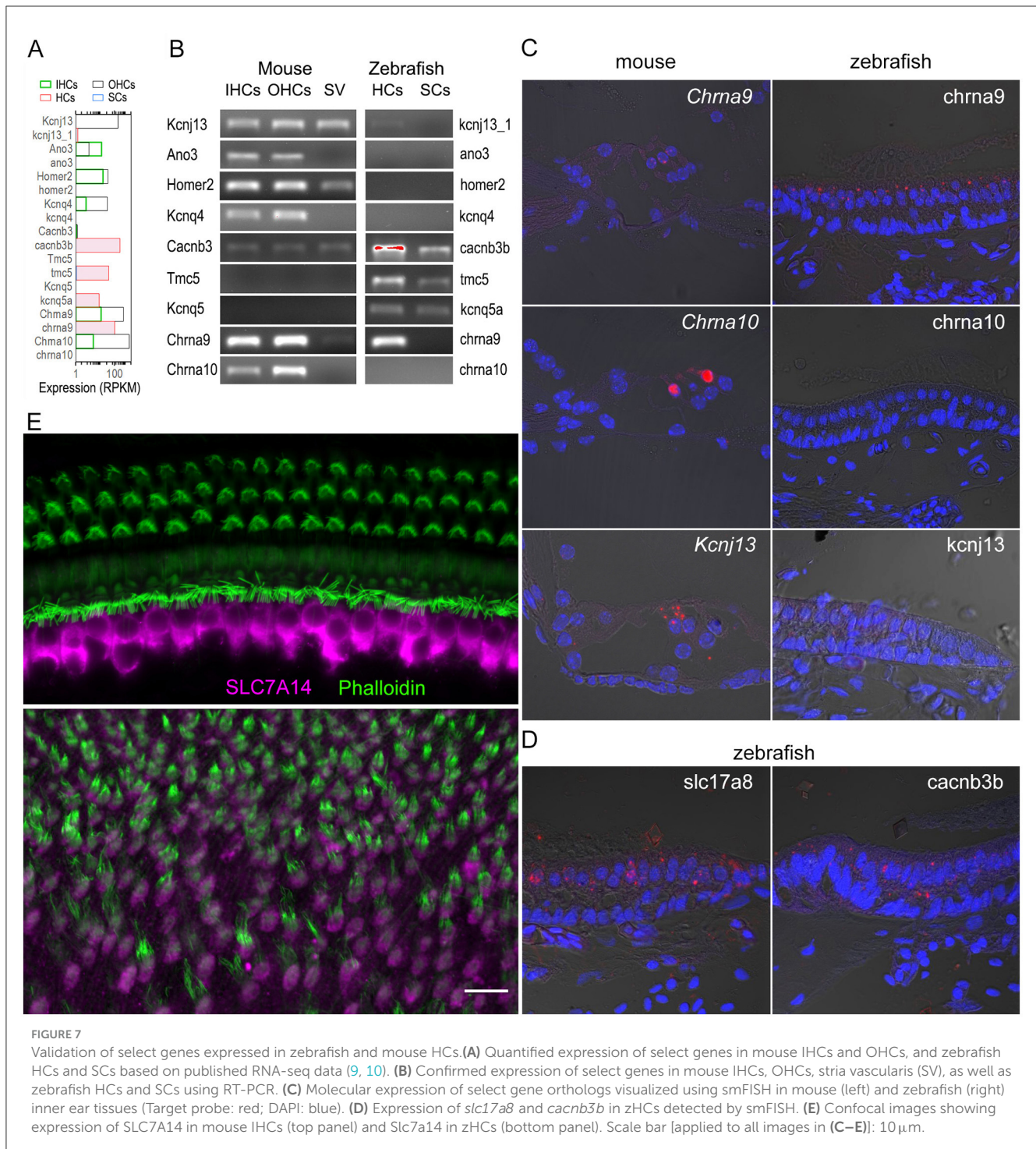
Common expression of gene orthologs encoding transcriptional regulators

To identify possible regulatory mechanisms that maintain mature vertebrate HC phenotypes, common expression of genes with transcription-associated functions was examined. An inclusive list of over 2,300 “transcription factor” (TF) gene orthologs, curated in a previous publication (11) included those with functions such as regulatory region DNA binding, chromatin-mediated transcriptional regulation, nuclear binding activity, and similar functions. First, to understand the conserved transcriptomic signatures of vertebrate HCs, the high-confidence gene orthologs expressed in all HCs were examined as these TF genes are more likely to have conserved functions. A total of 400 high-confidence TF gene orthologs were expressed in all HCs, the top 130 (>10.0 RPKM in all HCs) are shown in Figure 6A. An enrichment



analysis, using the ShinyGO TF Targets database showed significant enrichment (FDR value < 0.05) of target genes in the ELK1, GABP, PEA3 (ETV4), SP1, and STAT1 pathways. Further comparison of similarities among the HC populations showed seven TF genes co-expressed in zHCs and IHCs (not OHCs), 17 TF genes co-expressed

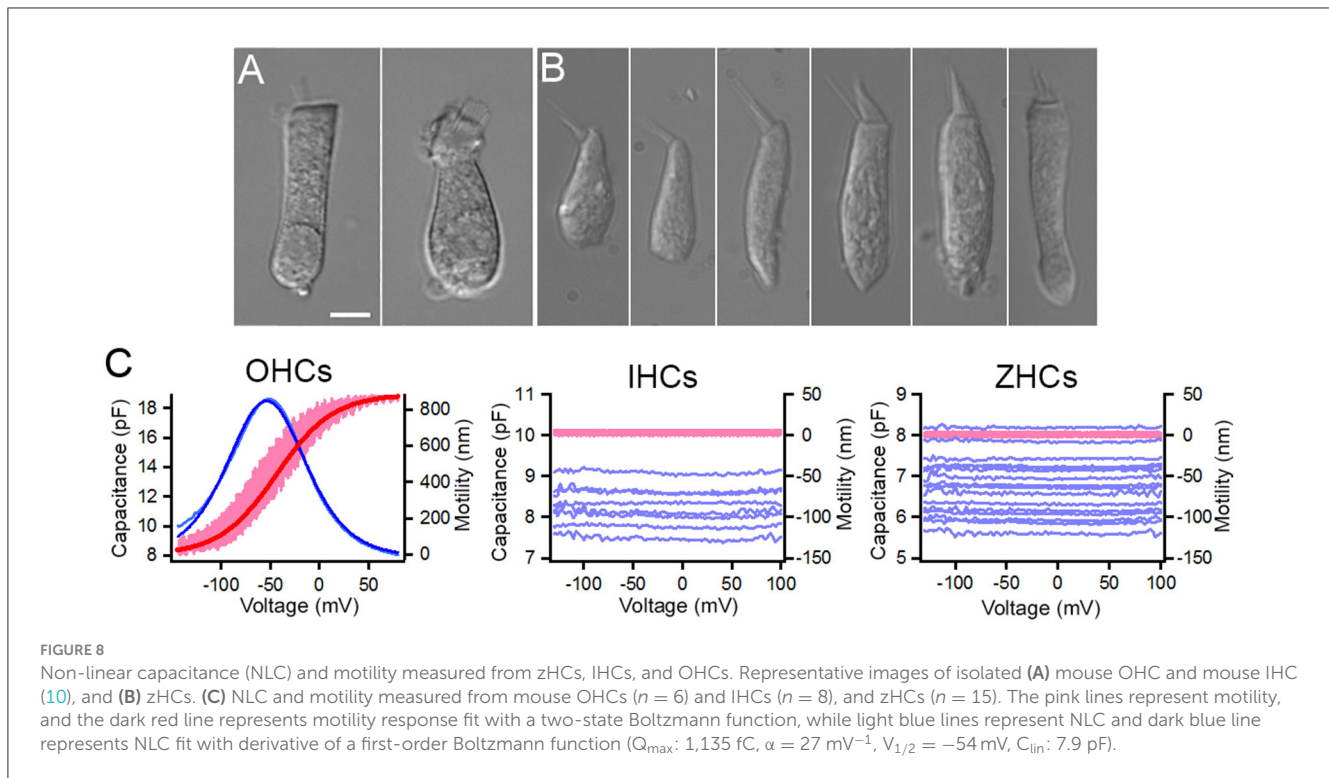
in zHCs and OHCs (not IHCs), and 28 TF genes co-expressed in IHCs and OHCs. For comparison, we also examined the top 20 expressed TF gene orthologs in each HC type (Figure 6B). There was notable overlap between those TF genes expressed in IHCs and OHCs, with 11 orthologs co-expressed in the list of the top 20 TFs.



Verification of gene expression in zebrafish and mouse inner ear cells

The expression of a subset of genes detected by RNA-seq (Figure 7A), selected based on unique expression patterns in zHCs, IHCs, and OHCs, was validated by RT-PCR (Figure 7B), smFISH (Figures 7C, D), and immunostaining (Figure 7E) in mouse and zebrafish tissue. As shown in Figures 7A, B, *Kcnj13*, *Ano3*, *Homer2*, *Kcnq4*, and *Chrna10* are expressed in mouse HCs. However, the

corresponding orthologs have little to no measurable expression in zHCs. Positive labeling with smFISH also showed *Kcnj13* mRNA expression in OHCs, with lower expression observed in IHCs, and minimal *kcnj13* expression in zHCs (Figure 7C). Conversely, expression of *Cacnb3* in IHCs and OHCs is quite low, relative to the high-level expression of the ortholog *cacnb3b* in zHCs (Figures 7B, D). Gene orthologs uniquely expressed in zHCs include *tmc5* and *kcnq5a* (Figure 7B). Expression of genes encoding cholinergic receptors *Chrna9* and *Chrna10* in both IHCs



and OHCs differs from the sole expression of *chrna9* in zHCs (Figures 7A–C). Comparatively, *slc17a8*, which encodes a vesicular glutamate transporter, is highly expressed in zHCs (Figure 7D), similar to expression of the ortholog *Slc17a8* in mammalian HCs (47). Finally, we used immunostaining to examine expression of SLC7A14, a protein that is evolutionarily conserved and expressed in photoreceptors, subcortical neurons, and vertebrate HCs (10, 48, 49). Loss of function of this gene leads to auditory neuropathy and retinitis pigmentosa in mice and humans (50). As shown in Figure 7E, SLC7A14 is robustly and specifically expressed in adult mammalian IHCs, while the ortholog, *Slc7a14*, is highly expressed in zHCs. Therefore, this protein-coding gene ortholog can serve as a marker for all HCs in non-mammals and IHCs in adult mammals.

Electromotility and nonlinear capacitance are properties unique to mammalian OHCs

Prestin, encoded by *Slc26a5*, is the motor protein that drives electromotility of mammalian OHCs. A prestin ortholog, *zprest*, was detected from the inner ear tissue of zebrafish (51). We examined *Slc26a5* expression in zebrafish and mouse HCs. As shown in Figure 4B, *Slc26a5* is highly expressed in OHCs and weakly expressed in IHCs with a ratio difference (in log₂ scale) of ~ 29 . Weak expression of *slc26a5* is detected in zHCs. Although non-linear capacitance (NLC), an electrical signature of electromotility, was detected in a cell line transfected with the *zprest* ortholog (51, 52), motility and NLC have never been measured from zHCs. We measured motility and NLC simultaneously from zHCs, with similar measurements from OHCs as a positive control and IHCs as a negative control. Zebrafish

HCs in utricle, saccule, and lagena have differing cell morphologies, with representative images shown in Figures 8A, B. Moreover, even within the same end organ, HCs located in striolar and extrastriolar regions differ in morphology and electrophysiology (53). We measured motility and NLC from 15 zHCs with different morphologies to capture regional diversity. While OHCs show robust voltage-dependent motility and large bell-shaped NLC, the zHCs do not show any signs of electromotility (Figure 8C). Capacitance response was also flat with no apparent voltage-dependence within the voltage range measured, which is somewhat different from a weak voltage-dependent response seen in *slc26a5*-transfected cell lines (51, 52). Similar to zHCs, IHCs also do not show any signs of motility and NLC, despite weak expression of *Slc26a5* in IHCs.

Discussion

The challenges of depicting the molecular signatures underlying HC physiology in mammals are numerous, thus, non-mammalian model systems, including zebrafish and chicken, have become useful to explore processes such as HC development and regeneration. Numerous studies previously characterized the gene expression profiles of vertebrate inner ear HCs (9, 54–56), including some of the first studies to isolate and sequence pure populations of mammalian IHCs and OHCs (10, 15). More recently, single-cell RNA-seq analyses of vertebrate inner ear HC populations have exponentially increased our knowledge of the transcriptomic signatures of these specialized sensory cells. Additionally, some studies have compared gene expression homology among avian and mammalian inner ear cells, though they were not HC-type specific (57). We examined

the homology of mouse cochlear IHCs and OHCs, and zebrafish inner ear HCs based on the expression of protein-coding gene orthologs among the cell populations. Thus, our study provides a novel comparative dataset to further the utility of zebrafish as a model for exploring mammalian HC function. Notably, common and uniquely expressed gene orthologs in mouse and zHCs, reveal transcriptomic signatures underlying phenotypic cellular specializations.

Shared and unique expression of gene orthologs reveals conserved transcriptomic signatures underlying vertebrate HC specialization

To aid in understanding some of the molecular signatures common and unique to inner ear HCs, we first compared expression patterns of protein-coding gene orthologs among each cell population. While the total number of genes in zHCs is greater, due to paralogous genes, the total percentage of gene orthologs expressed in each HC population accounted for about 62 to 65 percent of the total protein-coding gene orthologs. The shared expression of genes in homologous cell populations are more likely those associated with transcriptional regulation or metabolic pathways, while there may be greater divergence in expression of genes in cellular communication (58). When examining the number of commonly expressed genes among the distinct HC populations, mammalian IHCs and OHCs shared the highest number of expressed genes. Though surprisingly, OHCs and zHCs shared more commonly expressed genes than IHCs and zHCs. Perhaps the phenotypic diversity among zHCs is captured both in the shared overlap with OHCs with their unique features including electromotility, and IHCs as the true sensory cell of the auditory system (59). Differential gene expression analyses showed a greater number of genes upregulated in zHCs compared to either IHCs or OHCs, and over 2,800 uniquely expressed genes in zHCs. This suggests that some of these genes encode proteins specific to this cellular phenotype or are expressed paralogs that may have acquired a sub-function of the ancestral gene (60).

Differential gene expression reveals transcriptomic signatures of non-mammalian inner ear HCs and distinctive similarities to mammalian HCs

To provide a comprehensive overview of expressed protein-coding gene orthologs in zebrafish inner ear HCs compared to zSCs, we examined uniquely expressed and upregulated genes in zHCs. Compared to the transcriptomic signatures of zSCs, the zHCs uniquely expressed several genes or gene paralogs with known contribution to HC function. Furthermore, several of the highly expressed orthologs, including *gfi1aa*, *lhfp15a*, *myo6b*, *strc*, and *s100s* were recently described as molecular markers to delineate HC subtypes in the zebrafish inner ear (28), while others are known pan-HC genes or have been well-described as essential to HC

function. For example, the high-confidence orthologs *clic5a* (*Clic5*), encodes an intracellular chloride channel protein that localizes to the basal region of the hair bundle and loss-of-function is associated with dysmorphic stereocilia, and vestibular and hearing dysfunction (61). The *cib3* ortholog, encoding calcium-binding protein, has been shown to be co-expressed with *tmc1* in the zebrafish inner ear HCs, with the ortholog *Cib3* required for mechanotransduction in cochlear HCs (62–64). Expression of the gene orthologs *anxa5a* and *Anxa5* is highly conserved among vertebrate HCs, despite unknown functional significance of the protein in auditory HCs (65).

Expression of gene orthologs among zebrafish and mouse HCs reveals molecular signatures underlying sensory HC functional specialization

To further delineate the common transcriptomic signatures underlying vertebrate HC specialization, we compared expression of gene orthologs encoding functional HC proteins. For example, *Otof* (*otofa/b*), *Slc1a3* (*slc1a3a*), *Slc17a8* (*slc17a8*), and *Slc7a14* (*slc7a14b*) are highly expressed in zHCs and IHCs. *Slc26a5*, encoding the motor protein prestin (66), is highly expressed in OHCs and detected at similarly low levels in IHCs and zHCs (*slc26a5*). Subsequently, we demonstrated here that zHCs do not exhibit properties of electromotility.

A great degree of conserved expression was observed among those genes orthologs encoding stereocilia-associated proteins, as over 75 percent of the genes examined were expressed in all HCs. There are few distinct differences in expression, for example *actn4* and *vill* were not detected in zHC, while both IHCs and OHCs expressed the orthologs *Actn4* and *Vill*. The absence of conserved expression in zHCs is surprising, as the actin crosslinker proteins encoded by these orthologs were also previously detected in chicken HC stereocilia (29, 67). Conversely, other genes were highly expressed only in zHCs, such as *capza1a* and *1b*, while a related ortholog *Capzb* (*capzb*) was highly expressed in all HCs. CAPZ, a heterodimeric capping protein regulating stereocilia length and width in chick and mouse cochlear and utricle HCs, can consist of CAPZA or CAPZB subunits (67). This warrants further exploration of the composition of these Capz subunits in zHCs and whether their interactions with other stereocilia-associated proteins such as Grxcr1, Eps8l2, Eps8/Eps8b, and Twf2a/Twf2b are conserved.

In zebrafish and mouse HCs, there was also a high degree of conserved gene expression encoding the mechanotransduction components. TMC1 and TMC2 are subunits of a transmembrane mechanosensitive ion channel that mediates mechanotransduction in vertebrate HCs. These TMC proteins, together with other proteins such as calcium and integrin binding 2 and 3 (CIB2/CIB3), accessory protein LHFPL5, and the tip-link PCDH15/CDH23 complex, are essential for mechanosensory transduction of HCs (62, 68). Zebrafish HCs expressed *ush1c*, *tmie*, *pcdh15a/b*, and *lhfp15a*, but not the paralog *lhfp15b*, while mouse HCs expressed the orthologs *Ush1c*, *Tmie*, *Pcdh15*, and *Lhfp15*, respectively. Notably, zHCs expressed *tmc1*, *tmc2a*, and *tmc2b*, while IHCs and OHCs expressed only *Tmc1*. *Cib2* was highly expressed in

IHCs and OHCs, while both *cib2* and *cib3* were expressed in zHCs. Patterned co-expression of *tmc* subtypes with *cib2* and *cib3* among extrastriolar and striolar zHCs was recently described (64). Describing the identities and functional interactions among the components of the mechanotransduction channel in stereocilia continues to be an area of research interest.

Differential expression of ion channels among vertebrate HC populations has also been an ongoing area of inquiry, often further complicated by the many splice variants encoded by ion channel genes and the subunit composition of functional ion channels. We found that zHCs, compared to their mammalian counterparts, have a more diversified pattern of expression of ion channel genes, many of which are paralogous genes. It is unclear whether the expressed genes are redundant or if the protein encoded by a gene paralog became functional during evolution, though it should not be assumed that it retained the same molecular function (25). For example, zHCs express *kcnn1a* and *kcnn1b*, along with the paralog *kcnn2*. The ortholog *Kcnn1* has low expression in IHCs and OHCs, and *Kcnn2* is highly expressed in OHCs. *Kcnn2* encodes a calcium-activated potassium channel (SK2) which, along with $\alpha 9\alpha 10$ -containing ionotropic receptors, contributes to post-synaptic organization and cholinergic inhibition of efferent synaptic cisterns of mouse OHCs (69). Related expression patterns among zHCs include the differential expression of paralogous genes encoding the cholinergic receptor nicotinic (nAChR) $\alpha 9$ and $\alpha 10$ subunits. Both *Chrna9* and *Chrna10* are expressed in IHCs and OHCs, while only *chrna9* is expressed in zHCs. Consistent with mammalian expression, *Chrna9* and *Chrna10* are expressed by both short and tall HCs in the chicken cochlea (70). In birds and mammals, the $\alpha 9$ nAChRs are functionally coupled to SK2 potassium channels in HCs, and SK1 and SK2 are often co-expressed in the brain and can form heteromeric channels (71–73). The functional properties of the co-expressed paralogous SK channels and nAChRs in zHCs warrants further investigation, especially considering the greater sequence divergence among the HC $\alpha 9\alpha 10$ nAChRs across species (74). However, *Chrna10* appears to be an adaptation of both avians and mammals.

While many of these protein-coding gene orthologs may have conserved function in vertebrate HCs, there are other unique properties in non-mammalian HCs, such as electrical resonance, that may be attributed to some of the uniquely expressed ion channel genes. This process relies on electrical resonance properties that arise from the interplay of voltage-gated calcium channels and BK channels, together with membrane properties. For example, *cacnb3b* was strongly expressed in zHCs, compared to mild expression of *Cacnb3* in mouse HCs. Similarly, *kcnma1a*, encoding a large-conductance calcium activated potassium (BK) channel, was strongly expressed in zHCs, like the orthologous gene *kcnma1* (*cslo1*) detected in both tall and short chicken HCs (70). The high-level expression of these genes in zHCs, and not in mouse HCs, may contribute to the differential physiological properties underlying frequency tuning in non-mammalian vertebrate HCs. Differential expression of BK channel isoforms along chicken basilar papilla HCs mediates tonotopic frequency sensitivity, and knockdown of *kcnma1a* encoded BK channel expression increased auditory thresholds in larval zebrafish (75, 76). Whereas in mammals, BK knockout mice showed normal cochlear function and increased resistance to noise-induced hearing loss (77).

The unique contributions of the ion channels encoded by *cacnb3b* and its interplay with expressed isoforms encoded by *kcnma1a* in mediating electrical resonance of zHCs warrants further investigation. Furthermore, exploring the physiologic contributions of ion channels encoded by other uniquely expressed genes in zHCs may further our understanding of the divergent specializations in non-mammalian HCs.

Comparative transcriptomic analysis reinforces the utility of the zebrafish model for exploring hearing loss phenotypes and mechanisms of HC regeneration

While this study included only a subset of genes known to be associated to hearing loss phenotypes, those identified as one-to-one orthologs are more likely to have conserved functions. Considering this homology, characterization of induced gain or loss of function variants in zebrafish may be achieved more efficiently than mammalian models, allowing the molecular dysfunctions underlying hearing loss phenotypes to be further elucidated. For example, the lysosomal SLC transporter encoded by the orthologs *Slc7a14* and *slc7a14b* is highly expressed in IHCs and zHCs, respectively, and loss of function causes progressive auditory neuropathy and retinopathy (50). A recent study suggested that the SLC7A14 transporter had amino acid-sensing activity and mediated lysosomal uptake of GABA and subsequent inhibition of mTORC2 in hepatocytes (78). With its distinctive expression in HCs the molecular function of SLC7A14 can be examined using a zebrafish model. The utility of the zebrafish model is evidenced by the experimental validation of numerous auditory phenotypes and syndromic diseases, investigation of genes regulating HC development or function, and exploration of molecular therapies targeting pathogenic variants (4, 79–81).

Finally, analysis of the orthologous TFs regulating gene expression in mature mouse and zebrafish inner ear HCs further elucidated key molecular similarities and differences in these cell populations. While several of the commonly expressed genes are categorized as basal cell TFs, some are well characterized HC TF genes including *Eya1*, *Gata3*, *Pou4f3*, *Nr2f6*, *Sox2*, and others (82). Among the top expressed TF genes in HCs, were several regulated by SP1 which is known to induce transcriptional responses to physiologic or pathologic stimuli. Upregulation of SP1 and subsequent up or downregulation of target genes protected cochlear HCs from oxidative damage (83). STAT1 target genes, which regulate processes such as cell cycle arrest and immune response, were also enriched among all HCs. Decreased expression of STAT1 target genes reduced cisplatin-mediated apoptosis and aminoglycoside-induced inflammation in the mammalian cochlea (84, 85). More recent findings showed the therapeutic effects of compounds that ameliorate ototoxic drug-induced damage to the mouse cochlea and zebrafish lateral line HCs via regulation of STAT1 and STAT3 signaling (86, 87). *Stat3* (*stat3*) had lower expression in all HCs, while *stat1a* was more highly expressed in zHCs and zSCs. Given the interplay between STAT1 and STAT3 target genes and pathways, further study to elaborate why these STAT1 target genes are upregulated in all HCs, as well as the

regulatory activity of Stat1 in zHCs warrants further exploration. Another group of enriched TFs included ETV target genes; ETV TFs ETV4 and ETV5 are regulated downstream of mesenchymal FGF signaling to regulate cochlear length during development (88). Both zHCs and zSCs express *etv4* (*pea3*); upregulation of FGF signaling via Wnt activation significantly upregulated *etv4*, and subsequently induced cell proliferation in lateral line neuromasts (89). Interestingly, we found that *Etv5* (*etv5a/b*) was expressed in adult mouse and zHCs, however, the role of the ETV TFs in maintaining the adult sensory epithelia is unclear.

Continued exploration of the transcriptional landscapes regulating the mature HC phenotype will further the pursuit to regenerate adult mammalian HCs. Unlike their adult mammalian counterparts, mature zebrafish and chicken HCs retain the ability to regenerate by conversion from SCs to restore function after damage (90). Regeneration has been widely studied in zebrafish lateral line HCs and some of the molecular mechanisms regulating this process have been successfully utilized to induce regeneration of neonate mammalian HCs (91, 92). Although overexpression of a cocktail of TFs can convert SCs to HCs in adult mammals, the challenge to fully convert these to mature, functional HCs remains (93). Additional analyses, which correlate gene expression profiles during zHC regeneration, to both developing and mature mammalian HC gene expression profiles, will provide further clues to HC regeneration in adult mammals (94). Thus, the presented dataset, including expressed TF gene orthologs in mature inner ear HCs, may serve as a transcriptomic guide for regenerative studies.

Limitations

We recognize that describing functional homology among vertebrate HCs based on transcriptomic analyses is not without its caveats. Firstly, gene expression is not equivalent to protein expression, thus, further proteomic analysis of these and other vertebrate HC populations will further support shared and unique molecular functions. Single cell proteomic studies can reveal cell type-specific expression, developmental changes in expression, or post-translational modification of proteins, which can be highly informative of biological processes underlying HC function (95). To complement transcriptomic profiling, ongoing experiments, employing recent advances in single-cell proteomics, will identify and quantify proteins enriched in mouse and zebrafish HCs. Secondly, the original RNA-seq analysis of isolated zHCs were pooled from the utricle, saccule, and lagena, thus distinct gene expression patterns among the zHC subtypes with auditory and vestibular functions are not exhibited in this study. Recent transcriptomic profiling of adult zebrafish inner ear revealed cellular subtypes among HCs, further delineating the functions of the sensory epithelia (28). Future analysis of orthologous gene expression, defining conserved and unique HC subtypes, is increasingly possible as single-cell RNA-seq technologies continue to improve our abilities to isolate and sequence mature mouse inner ear HCs. Importantly, these single-cell studies are informed by prior transcriptomic analyses using bulk RNA-seq which have several advantages including greater hair cell sample size and depth of coverage.

Conclusion

While we focused most of this analysis on genes with known HC functions, this is by no means a comprehensive analysis of protein-coding orthologs that may contribute to ion transport, mechanotransduction, synaptic signaling, or maintenance and regeneration of the sensory HCs. Importantly, these data provide a resource for further exploring the molecular signatures underlying HC-specific functions in zebrafish and mouse. Additionally, this work creates a foundation for future comparisons of protein-coding gene ortholog expression in other species to further elucidate the conserved molecular signatures among vertebrate inner ear HCs.

Data availability statement

Previously published RNA-seq datasets were used in this comparative analysis and are accessible in online repositories. This includes transcriptomic data from adult zebrafish inner ear HCs and nonsensory supporting cells (NCBI SRP113243), and IHCs and OHCs from adult mouse cochlea (NCBI SRP133880).

Ethics statement

The animal study was approved by Creighton University Institutional Animal Care and Use Committee. The study was conducted in accordance with the local legislation and institutional requirements.

Author contributions

KG: Validation, Writing – review & editing, Writing – original draft, Visualization, Methodology, Investigation, Formal analysis, Data curation, Conceptualization. HL: Writing – review & editing, Visualization, Methodology, Investigation. KY: Writing – review & editing, Visualization, Methodology, Investigation. YL: Writing – review & editing, Methodology, Investigation. LC: Writing – review & editing, Methodology, Investigation. KK: Writing – review & editing, Resources, Methodology. MZ: Writing – review & editing, Resources, Methodology. DH: Writing – review & editing, Writing – original draft, Visualization, Validation, Supervision, Resources, Project administration, Methodology, Funding acquisition, Conceptualization.

Funding

The author(s) declare financial support was received for the research, authorship, and/or publication of this article. This work has been supported by the NIH grant R01 DC004696 (to DH) from the NIDCD. The Imaging and Molecular Biology Cores at the Translational Hearing Research Center of Creighton University School of Medicine are supported by NIH grant 1P20GM139762 from the NIGMS and by Bellucci Depauli Family

Foundation. The content is solely the responsibility of the authors and does not necessarily represent the official views of the NIH.

Conflict of interest

The authors declare that the research was conducted in the absence of any commercial or financial relationships that could be construed as a potential conflict of interest.

The author(s) declared that they were an editorial board member of Frontiers, at the time of submission. This had no impact on the peer review process and the final decision.

References

- Hudspeth AJ, Corey DP. Sensitivity, polarity, and conductance change in the response of vertebrate hair cells to controlled mechanical stimuli. *Proc Natl Acad Sci U S A*. (1977) 74:2407–11. doi: 10.1073/pnas.74.6.2407
- Fettiplace R, Fuchs PA. Mechanisms of hair cell tuning. *Annu Rev Physiol*. (1999) 61:809–34. doi: 10.1146/annurev.physiol.61.1.809
- Salvi JD, Ó Maoiléidigh D, Fabella BA, Tobin M, Hudspeth AJ. Control of a hair bundle's mechanosensory function by its mechanical load. *Proc Natl Acad Sci USA*. (2015) 112:E1000–E1009. doi: 10.1073/pnas.1501453112
- Nicolson T. The genetics of hair-cell function in zebrafish. *J Neurogenet*. (2017) 31:102–12. doi: 10.1080/01677063.2017.1342246
- Fettiplace R. Diverse mechanisms of sound frequency discrimination in the vertebrate cochlea. *Trends Neurosci*. (2020) 43:88–102. doi: 10.1016/j.tins.2019.12.003
- Liberman MC, Gao J, He DZZ, Wu X, Jia S, Zuo J. Prestin is required for electromotility of the outer hair cell and for the cochlear amplifier. *Nature*. (2002) 419:300–4. doi: 10.1038/nature01059
- Dallos P, Wu X, Cheatham MA, Gao J, Zheng J, Anderson CT, et al. Prestin-based outer hair cell motility is necessary for mammalian cochlear amplification. *Neuron*. (2008) 58:333–9. doi: 10.1016/j.neuron.2008.02.028
- Hudspeth AJ. Integrating the active process of hair cells with cochlear function. *Nat Rev Neurosci*. (2014) 15:600–14. doi: 10.1038/nrn3786
- Barta CL, Liu H, Chen L, Giffen KP, Li Y, Kramer KL, et al. RNA-seq transcriptomic analysis of adult zebrafish inner ear hair cells. *Sci Data*. (2018) 5:180005. doi: 10.1038/sdata.2018.5
- Li Y, Liu H, Giffen KP, Chen L, Beisel KW, He DZZ. Transcriptomes of cochlear inner and outer hair cells from adult mice. *Sci Data*. (2018) 5:180199. doi: 10.1038/sdata.2018.199
- Giffen KP, Liu H, Kramer KL, He DZ. Expression of protein-coding gene orthologs in zebrafish and mouse inner ear non-sensory supporting cells. *Front Neurosci*. (2019) 13:1117. doi: 10.3389/fnins.2019.01117
- Cunningham F, Allen JE, Allen J, Alvarez-Jarreta J, Amode MR, Armean IM, et al. Ensembl 2022. *Nucleic Acids Res*. (2022) 50:D988–95. doi: 10.1093/nar/gkab1049
- Zerbino DR, Achuthan P, Akanni W, Amode MR, Barrell D, Bhai J, et al. Ensembl 2018. *Nucleic Acids Res*. (2018) 46:D754–61. doi: 10.1093/nar/gkx1098
- He DZZ, Zheng J, Edge R, Dallos P. Isolation of cochlear inner hair cells. *Hear Res*. (2000) 145:156–60. doi: 10.1016/S0378-5955(00)00084-8
- Liu H, Pecka JL, Zhang Q, Soukup GA, Beisel KW, He DZZ. Characterization of transcriptomes of cochlear inner and outer hair cells. *J Neurosci*. (2014) 34:11085–95. doi: 10.1523/JNEUROSCI.1690-14.2014
- Ge SX, Son EW, Yao R. iDEP: an integrated web application for differential expression and pathway analysis of RNA-Seq data. *BMC Bioinform*. (2018) 19:534. doi: 10.1186/s12859-018-2486-6
- Ge SX, Jung D, Yao R. ShinyGO: a graphical gene-set enrichment tool for animals and plants. *Bioinformatics*. (2020) 36:2628–9. doi: 10.1093/bioinformatics/btz931
- Davis MW, Jorgensen EM, ApE, A plasmid editor: a freely available DNA manipulation and visualization program. *Front Bioinform*. (2022) 2:818619. doi: 10.3389/fbinf.2022.818619
- Salehi P, Nelson CN, Chen Y, Lei D, Crish SD, Nelson J, et al. Detection of single mRNAs in individual cells of the auditory system. *Hear Res*. (2018) 367:88–96. doi: 10.1016/j.heares.2018.07.008
- Wang X, Yang S, Jia S, He DZZ. Prestin forms oligomer with four mechanically independent subunits. *Brain Res*. (2010) 1333:28–35. doi: 10.1016/j.brainres.2010.03.070
- Santos-Sacchi J, Kakehata S, Kikuchi T, Katori Y, Takasaka T. Density of motility-related charge in the outer hair cell of the guinea pig is inversely related to best frequency. *Neurosci Lett*. (1998) 256:155–8. doi: 10.1016/S0304-3940(98)00788-5
- Jia S, He DZZ. Motility-associated hair-bundle motion in mammalian outer hair cells. *Nat Neurosci*. (2005) 8:1028–34. doi: 10.1038/nn1509
- Ashmore JF. Transducer motor coupling in cochlear outer hair cells. In: Wilson JP, Kemp DT, editor. *Cochlear Mechanisms: Structure, Function, and Models*. Boston, MA: Springer US (1989). p. 107–114. doi: 10.1007/978-1-4684-5640-0_13
- Santos-Sacchi J. Reversible inhibition of voltage-dependent outer hair cell motility and capacitance. *J Neurosci*. (1991) 11:3096–110. doi: 10.1523/JNEUROSCI.11-10-03096.1991
- Koonin EV. Orthologs, paralogs, and evolutionary genomics. *Annu Rev Genet*. (2005) 39:309–38. doi: 10.1146/annurev.genet.39.073003.114725
- Erickson T, Nicolson T. Identification of sensory hair-cell transcripts by thiouracil-tagging in zebrafish. *BMC Genomics*. (2015) 16:842. doi: 10.1186/s12864-015-2072-5
- Erickson T, Pacentine IV, Venuto A, Clemens R, Nicolson T. The lhfp15 ohnologs lhfp15a and lhfp15b are required for mechanotransduction in distinct populations of sensory hair cells in zebrafish. *Front Mol Neurosci*. (2019) 12:320. doi: 10.3389/fnmol.2019.00320
- Shi T, Beaulieu MO, Saunders LM, Fabian P, Trapnell C, Segil N, et al. Single-cell transcriptomic profiling of the zebrafish inner ear reveals molecularly distinct hair cell and supporting cell subtypes. *Elife*. (2023) 12:e82978. doi: 10.7554/eLife.82978
- Shin JB, Krey JF, Hassan A, Metlagel Z, Tauscher AN, Pagana JM, et al. Molecular architecture of the chick vestibular hair bundle. *Nat Neurosci*. (2013) 16:365–74. doi: 10.1038/nn.3312
- Krey JF, Barr-Gillespie PG. Molecular composition of vestibular hair bundles. *Cold Spring Harb Perspect Med*. (2018) 9:a033209. doi: 10.1101/cshperspect.a033209
- Tian C, Kim YJ, Hali S, Choo OS, Lee JS, Jung SK, et al. Suppressed expression of LDHB promotes age-related hearing loss via aerobic glycolysis. *Cell Death Dis*. (2020) 11:375. doi: 10.1038/s41419-020-2577-y
- Caprara GA, Peng AW. Mechanotransduction in mammalian sensory hair cells. *Mol Cell Neurosci*. (2022) 120:103706. doi: 10.1016/j.mcn.2022.103706
- Kawashima Y, Géléc GSG, Kurima K, Labay V, Lelli A, Asai Y, et al. Mechanotransduction in mouse inner ear hair cells requires transmembrane channel-like genes. *J Clin Invest*. (2011) 121:4796–809. doi: 10.1172/JCI60405
- Kim KX, Beurg M, Hackney CM, Furness DN, Mahendrasingam S, Fettiplace R. The role of transmembrane channel-like proteins in the operation of hair cell mechanotransducer channels. *J Gen Physiol*. (2013) 142:493–505. doi: 10.1085/jgp.2013.11068

Publisher's note

All claims expressed in this article are solely those of the authors and do not necessarily represent those of their affiliated organizations, or those of the publisher, the editors and the reviewers. Any product that may be evaluated in this article, or claim that may be made by its manufacturer, is not guaranteed or endorsed by the publisher.

Supplementary material

The Supplementary Material for this article can be found online at: <https://www.frontiersin.org/articles/10.3389/fneur.2024.1437558/full#supplementary-material>

35. Pan B, Géléoc GS, Asai Y, Horwitz GC, Kurima K, Ishikawa K, et al. TMC1 and TMC2 are components of the mechanotransduction channel in hair cells of the mammalian inner ear. *Neuron*. (2013) 79:504–15. doi: 10.1016/j.neuron.2013.06.019
36. Kalay E, Li Y, Uzumcu A, Uyguner O, Collin RW, Caylan R, et al. Mutations in the lipoma HMGIC fusion partner-like 5 (LHFPL5) gene cause autosomal recessive nonsyndromic hearing loss. *Hum Mutat*. (2006) 27:633–9. doi: 10.1002/humu.20368
37. Xiong W, Grillet N, Elledge HM, Wagner TFJ, Zhao B, Johnson KR, et al. TMHS is an integral component of the mechanotransduction machinery of cochlear hair cells. *Cell*. (2012) 151:1283–95. doi: 10.1016/j.cell.2012.10.041
38. Zhao B, Wu Z, Grillet N, Yan L, Xiong W, Harkins-Perry S, et al. TMIE is an essential component of the mechanotransduction machinery of cochlear hair cells. *Neuron*. (2014) 84:954–67. doi: 10.1016/j.neuron.2014.10.041
39. Wu Z, Grillet N, Zhao B, Cunningham C, Harkins-Perry S, Coste B, et al. Mechanosensory hair cells express two molecularly distinct mechanotransduction channels. *Nat Neurosci*. (2017) 20:24–33. doi: 10.1038/nn.4449
40. Kros C. Physiology of mammalian cochlear HCs. In *The Cochlea: Springer Handbook of Auditory Research*. New York: Springer-Verlag (1996). p. 318–385. doi: 10.1007/978-1-4612-0757-3_6
41. Mittal R, Aranke M, Debs LH, Nguyen D, Patel AP, Grati M, et al. Indispensable role of ion channels and transporters in the auditory system. *J Cell Physiol*. (2017) 232:743–58. doi: 10.1002/jcp.25631
42. Roux I, Saffedine S, Nouvian R, Grati M, Simmler MC, Bahloul A, et al. Otoferlin, defective in a human deafness form, is essential for exocytosis at the auditory ribbon synapse. *Cell*. (2006) 127:277–89. doi: 10.1016/j.cell.2006.08.040
43. Ruel J, Emery S, Nouvian R, Bersot T, Amilhon B, Rybroek JMV, et al. Impairment of SLC17A8 encoding vesicular glutamate transporter-3, VGLUT3, underlies nonsyndromic deafness DFNA25 and inner hair cell dysfunction in null mice. *Am J Hum Genet*. (2008) 83:278–92. doi: 10.1016/j.ajhg.2008.07.008
44. Elgoyhen AB, Johnson DS, Boulter J, Vetter DE, Heinemann S. Alpha 9: an acetylcholine receptor with novel pharmacological properties expressed in rat cochlear hair cells. *Cell*. (1994) 79:705–15. doi: 10.1016/0092-8674(94)90555-X
45. Vetter DE, Katz E, Maison SF, Taranda J, Turcan S, Ballesteros J, et al. The $\alpha 10$ nicotinic acetylcholine receptor subunit is required for normal synaptic function and integrity of the olivocochlear system. *Proc Natl Acad Sci*. (2007) 104:20594–9. doi: 10.1073/pnas.0708545105
46. Cartagena-Rivera AX, Le Gal S, Richards K, Verpy E, Chadwick RS. Cochlear outer hair cell horizontal top connectors mediate mature stereocilia bundle mechanics. *Sci Adv*. (2019) 5:eaat9934. doi: 10.1126/sciadv.aat9934
47. Liu H, Giffen KP, Chen L, Henderson HJ, Cao TA, Kozeny GA, et al. Molecular and cytological profiling of biological aging of mouse cochlear inner and outer hair cells. *Cell Rep*. (2022) 39:110665. doi: 10.1016/j.celrep.2022.110665
48. Lein ES, Hawrylycz MJ, Ao N, Ayres M, Bensinger A, Bernard A, et al. Genome-wide atlas of gene expression in the adult mouse brain. *Nature*. (2007) 445:168–76. doi: 10.1038/nature05453
49. Jin Z-B, Huang XF, Lv JN, Xiang L, Li DQ, Chen J, et al. SLC7A14 linked to autosomal recessive retinitis pigmentosa. *Nat Commun*. (2014) 5:3517. doi: 10.1038/ncomms4517
50. Giffen KP, Li Y, Liu H, Zhao XC, Zhang CJ, Shen RJ, et al. Mutation of SLC7A14 causes auditory neuropathy and retinitis pigmentosa mediated by lysosomal dysfunction. *Sci Adv*. (2022) 8:eabk0942. doi: 10.1126/sciadv.abk0942
51. Albert JT, Winter H, Schaechinger TJ, Weber T, Wang X, He DZZ, et al. Voltage-sensitive prestin orthologue expressed in zebrafish hair cells. *J Physiol*. (2007) 580:451–61. doi: 10.1113/jphysiol.2007.127993
52. Tan X, Pecka JL, Tang J, Okoruwa OE, Zhang Q, Beisel KW, et al. From zebrafish to mammal: functional evolution of prestin, the motor protein of cochlear outer hair cells. *J Neurophysiol*. (2011) 105:36–44. doi: 10.1152/jn.00234.2010
53. Olt J, Johnson SL, Marcotti W. In vivo and in vitro biophysical properties of hair cells from the lateral line and inner ear of developing and adult zebrafish. *J Physiol*. (2014) 592:2041–58. doi: 10.1113/jphysiol.2013.265108
54. Cai T, Jen HI, Kang H, Klisch TJ, Zoghbi HY, Groves AK. Characterization of the transcriptome of nascent hair cells and identification of direct targets of the Atoh1 transcription factor. *J Neurosci*. (2015) 35:5870–83. doi: 10.1523/JNEUROSCI.5083-14.2015
55. Schrauwen I, Hasin-Brumshtein Y, Corneveaux JJ, Ohmen J, White C, Allen AN, et al. A comprehensive catalogue of the coding and non-coding transcripts of the human inner ear. *Hear Res*. (2016) 333:266–74. doi: 10.1016/j.heares.2015.08.013
56. Matern MS, Beirl A, Ogawa Y, Song Y, Paladugu N, Kindt KS, et al. Transcriptomic profiling of zebrafish hair cells using ribotag. *Front Cell Dev Biol*. (2018) 6:47. doi: 10.3389/fcell.2018.00047
57. Wu J, Zhang Y, Mao S, Li W, Li G, Li H, et al. Cross-species analysis and comparison of the inner ear between chickens and mice. *J Comp Neurol*. (2023) 531:1443–58. doi: 10.1002/cne.25524
58. Alam T, Agrawal S, Severin J, Young RS, Andersson R, Arner E, et al. Comparative transcriptomics of primary cells in vertebrates. *Genome Res*. (2020) 30:951–61. doi: 10.1101/gr.255679.119
59. Dallos P. The active cochlea. *J Neurosci*. (1992) 12:4575–85. doi: 10.1523/JNEUROSCI.12-12-04575.1992
60. Rohmann KN, Deitcher DL, Bass AH. Calcium-activated potassium (BK) channels are encoded by duplicate slo1 genes in teleost fishes. *Mol Biol Evol*. (2009) 26:1509–21. doi: 10.1093/molbev/msp060
61. Gagnon LH, Longo-Guess CM, Berryman M, Shin JB, Saylor KW, Yu H, et al. The chloride intracellular channel protein CLIC5 is expressed at high levels in hair cell stereocilia and is essential for normal inner ear function. *J Neurosci*. (2006) 26:10188–98. doi: 10.1523/JNEUROSCI.2166-06.2006
62. Liang X, Qiu X, Dionne G, Cunningham CL, Pucak ML, Peng G, et al. CIB2 and CIB3 are auxiliary subunits of the mechanotransduction channel of hair cells. *Neuron*. (2021) 109:2131–2149.e15. doi: 10.1016/j.neuron.2021.05.007
63. Giese AP, Weng WH, Kindt KS, Chang HH, Montgomery JS, Ratzan EM, et al. Complexes of vertebrate TMC1/2 and CIB2/3 proteins form hair-cell mechanotransduction cation channels. *Prepr Serv Biol*. (2023) 1:e89719. doi: 10.7554/eLife.89719
64. Smith ET, Sun P, Yu SK, Raible DW, Nicolson T. Differential expression of mechanotransduction complex genes in auditory/vestibular hair cells in zebrafish. *Front Mol Neurosci*. (2023) 16:1274822. doi: 10.3389/fnmol.2023.1274822
65. Krey JF, Drummond M, Foster S, Porsov E, Vijayakumar S, Choi D, et al. Annexin A5 is the most abundant membrane-associated protein in stereocilia but is dispensable for hair-bundle development and function. *Sci Rep*. (2016) 6:27221. doi: 10.1038/srep27221
66. Zheng J, Shen W, He DZ, Long KB, Madison LD, Dallos P. Prestin is the motor protein of cochlear outer hair cells. *Nature*. (2000) 405:149–55. doi: 10.1038/35012009
67. Avenarius MR, Krey JF, Dumont RA, Morgan CP, Benson CB, Vijayakumar S, et al. Heterodimeric capping protein is required for stereocilia length and width regulation. *J Cell Biol*. (2017) 216:3861–81. doi: 10.1083/jcb.201704171
68. Holt JR, Tobin M, Elferich J, Gouaux E, Ballesteros A, Yan Z, et al. Putting the pieces together: the hair cell transduction complex. *J Assoc Res Otolaryngol*. (2021) 22:601–8. doi: 10.1007/s10162-021-00808-0
69. Fuchs PA, Lehar M, Hiel H. Ultrastructure of cisternal synapses on outer hair cells of the mouse cochlea. *J Comp Neurol*. (2014) 522:717–29. doi: 10.1002/cne.23478
70. Janesick A, Scheibinger M, Benkafadar N, Kirti S, Ellwanger D, C., and Heller S. (2021). Cell-type identity of the avian cochlea. *Cell Rep*. 34:108900. doi: 10.1016/j.celrep.2021.108900
71. Dulon D, Luo L, Zhang C, Ryan AF. Expression of small-conductance calcium-activated potassium channels (SK) in outer hair cells of the rat cochlea. *Eur J Neurosci*. (1998) 10:907–15. doi: 10.1046/j.1460-9568.1998.00098.x
72. Matthews TM, Duncan RK, Zidanic M, Michael TH, Fuchs PA. Cloning and characterization of SK2 channel from chicken short hair cells. *J Comp Physiol A Neuroethol Sens Neural Behav Physiol*. (2005) 191:491–503. doi: 10.1007/s00359-005-0601-4
73. Carpaneto Freixas AE, Moglie MJ, Castagnola T, Salatino L, Domene S, Marcovich I, et al. Unraveling the molecular players at the cholinergic efferent synapse of the zebrafish lateral line. *J Neurosci*. (2021) 41:47–60. doi: 10.1523/JNEUROSCI.1772-20.2020
74. Marcovich I, Moglie MJ, Carpaneto Freixas AE, Trigiani AP, Franchini LF, Pätz PV, et al. Distinct evolutionary trajectories of neuronal and hair cell nicotinic acetylcholine receptors. *Mol Biol Evol*. (2020) 37:1070–89. doi: 10.1093/molbev/msz290
75. Rosenblatt KP, Sun ZP, Heller S, Hudspeth AJ. Distribution of Ca²⁺-activated K⁺ channel isoforms along the tonotopic gradient of the chicken's cochlea. *Neuron*. (1997) 19:1061–75. doi: 10.1016/S0896-6273(00)80397-9
76. Rohmann KN, Tripp JA, Genova RM, Bass AH. Manipulation of BK channel expression is sufficient to alter auditory hair cell thresholds in larval zebrafish. *J Exp Biol*. (2014) 217:2531–9. doi: 10.1242/jeb.103093
77. Pyott SJ, Meredith AL, Fodor AA, Vázquez AE, Yamoah EN, Aldrich RW. Cochlear function in mice lacking the BK channel alpha, beta1, or beta4 subunits. *J Biol Chem*. (2007) 282:3312–24. doi: 10.1074/jbc.M608726200
78. Jiang X, Liu K, Jiang H, Yin H, Wang E, Cheng H, et al. SLC7A14 imports GABA to lysosomes and impairs hepatic insulin sensitivity via inhibiting mTORC2. *Cell Rep*. (2023) 42:111984. doi: 10.1016/j.celrep.2022.111984
79. Blanco-Sánchez B, Clément A, Phillips JB, Westerfield M. Chapter 16 - Zebrafish models of human eye and inner ear diseases. In: Detrich HW, Westerfield M, Zon LI, editors. *Methods in Cell Biology*. Academic Press (2017). p. 415–467. doi: 10.1016/bs.mcb.2016.10.006
80. Pickett SB, Raible DW. Water waves to sound waves: using zebrafish to explore hair cell biology. *J Assoc Res Otolaryngol*. (2019) 20:1–19. doi: 10.1007/s10162-018-00711-1
81. Stemerink M, García-Bohórquez B, Schellens R, García-García G, Van Wijk E, Millan JM. Genetics, pathogenesis and therapeutic developments for Usher syndrome type 2. *Hum Genet*. (2022) 141:737–58. doi: 10.1007/s00439-021-02324-w
82. Elliott KL, Pavlínková G, Chizhikov VV, Yamoah EN, Fritsch B. Development in the mammalian auditory system depends on transcription factors. *Int J Mol Sci*. (2021) 22:4189. doi: 10.3390/ijms22084189

83. Li L, Xu K, Bai X, Wang Z, Tian X, Chen X. UCHL1 regulated by Sp1 ameliorates cochlear hair cell senescence and oxidative damage. *Exp Ther Med.* (2023) 25:94. doi: 10.3892/etm.2023.11793
84. Levano S, Bodmer D. Loss of STAT1 protects hair cells from ototoxicity through modulation of STAT3, c-Jun, Akt, and autophagy factors. *Cell Death Dis.* (2015) 6:e2019. doi: 10.1038/cddis.2015.362
85. Kaur T, Borse V, Sheth S, Sheehan K, Ghosh S, Tupal S, et al. Adenosine A1 receptor protects against cisplatin ototoxicity by suppressing the NOX3/STAT1 inflammatory pathway in the cochlea. *J Neurosci.* (2016) 36:3962–77. doi: 10.1523/JNEUROSCI.3111-15.2016
86. Yin H, Sun Y, Ya B, Guo Y, Zhao H, Zhang L, et al. Apelin-13 protects against cisplatin-induced ototoxicity by inhibiting apoptosis and regulating STAT1 and STAT3. *Arch Toxicol.* (2023) 97:2477–93. doi: 10.1007/s00204-023-03544-x
87. Yang H, Zong T, Liu J, Wang D, Gong K, Yin H, et al. Rutin attenuates gentamycin-induced hair cell injury in the zebrafish lateral line via suppressing STAT1. *Mol Neurobiol.* (2024) 2024:1–12. doi: 10.1007/s12035-024-04179-4
88. Ebeid M, Huh SH. Mesenchymal ETV transcription factors regulate cochlear length. *Hear Res.* (2020) 396:108039. doi: 10.1016/j.heares.2020.108039
89. Tang D, He Y, Li W, Li H. Wnt/ β -catenin interacts with the FGF pathway to promote proliferation and regenerative cell proliferation in the zebrafish lateral line neuromast. *Exp Mol Med.* (2019) 51:1–16. doi: 10.1038/s12276-019-0247-x
90. Choi S-W, Abitbol JM, Cheng AG. Hair cell regeneration: from animals to humans. *Clin Exp Otorhinolaryngol.* (2024) 17:1–14. doi: 10.21053/ceo.2023.01382
91. Ye Z, Su Z, Xie S, Liu Y, Wang Y, Xu X, et al. Yap-lin28a axis targets let7-Wnt pathway to restore progenitors for initiating regeneration. *Elife.* (2020) 9:e55771. doi: 10.7554/eLife.55771
92. Li X-J, Morgan C, Goff LA, Doetzlhofer A. Follistatin promotes LIN28B-mediated supporting cell reprogramming and hair cell regeneration in the murine cochlea. *Sci Adv.* (2022) 8:eabj7651. doi: 10.1126/sciadv.abj7651
93. Lee S, Song JJ, Beyer LA, Swiderski DL, Prieskorn DM, Acar M, et al. Combinatorial Atoh1 and Gfi1 induction enhances hair cell regeneration in the adult cochlea. *Sci Rep.* (2020) 10:21397. doi: 10.1038/s41598-020-78167-8
94. Baek S, Tran NT, Diaz DC, Tsai YY, Acedo JN, Lush ME, et al. Single-cell transcriptome analysis reveals three sequential phases of gene expression during zebrafish sensory hair cell regeneration. *Dev Cell.* (2022) 57:799–819.e6. doi: 10.1016/j.devcel.2022.03.001
95. Zhu Y, Scheibinger M, Ellwanger DC, Krey JF, Choi D, Kelly RT, et al. Single-cell proteomics reveals changes in expression during hair-cell development. *Elife.* (2019) 8:e50777. doi: 10.7554/eLife.50777